

On the creation of stagnation points near straight and sloped walls

T. Mullin^{a)}

Department of Physics and Astronomy, University of Manchester, Manchester M13 9PL, United Kingdom

J. J. Kobine

DAMTP, University of Cambridge, Cambridge CB3 9EW, United Kingdom

S. J. Tavener

Department of Math, Pennsylvania State University, University Park, Pennsylvania 16802

K. A. Cliffe

AEA Technology, Harwell, OX11 0RA, United Kingdom

Received 6 April 1999; accepted 5 October 1999

We report the results of an experimental and numerical study of the creation of stagnation points in a rotating cylinder of fluid where one endwall is rotated. Good agreement is found with previous results where the stagnation points are formed on the free core of the primary columnar vortex. The effect of adding a small cylinder along the center of the flow is then investigated and the phenomena are found to be robust despite the qualitative change in the boundary conditions. Finally, we show that sloping the inner cylinder has a dramatic effect on the recirculation such that it can either be intensified or suppressed. © 2000 American Institute of Physics. [S1070-6631(00)02601-5]

I. INTRODUCTION

The formation of stagnation points on the core of a confined columnar vortex in a cylindrical container of fluid, where one end rotates, was first investigated experimentally and numerically by Vogel.¹ The problem provides an example of a fluid flow where direct quantitative comparison can be made between the results of experiments and numerical calculations of the Navier–Stokes equations with realistic boundary conditions. Vogel found the base flow to consist of a large toroidal vortex with outward flow along the rotating endwall and a return along a tightly wound core. He observed that a delicate recirculation was created on the core of the vortex above a certain rotation rate of the endwall and confirmed his observations numerically. Vogel and others have likened the formation of the recirculation bubble to a weak version of the important, but as yet, unresolved problem of vortex breakdown. A discussion of these ideas is given by Lopez.²

The majority of subsequent research on the topic has been concerned with the same simple geometry of a cylinder of fluid where one end is made to rotate. The flow state can be considered to be defined in terms of two control parameters, the Reynolds number (R) and aspect ratio ($\Gamma = h/r$ where h is the height of the cylinder of radius r). Perhaps the most extensive experimental study was performed by Escudier³ who uncovered parameter ranges for the existence of single and multiple steady recirculations as well as unsteady flows. It was subsequently established by Tsitverblit⁴ that the appearance of the single steady recirculation is not an example of a hydrodynamic instability or bifurcation. Rather, it is the smooth development of one steady axisym-

metric flow from another when R is increased in an appropriate control parameter regime. Nevertheless, an understanding of the formation of the bubble is desirable since the stagnation point provides a focus for temporal instabilities which develop with further increase in R as discussed by Tsitverblit and Kit⁵ and Sorensen and Christensen.⁶

The experimental studies by Escudier have instigated many subsequent theoretical, experimental, and numerical investigations where the focus has primarily been on the possible links with vortex breakdown. In addition, studies of modified versions of the original problem have also been reported, including the effects of a free surface by Spohn, Mory, and Hopfinger⁷ and co- and counter-rotating the ends of the cylinder by Valentine and Jahnke⁸ and Lopez.⁹ One outcome of this research is that flow is steady and axisymmetric over a wide range of the control parameters, so that detailed numerical investigations of the bubble formation can be performed using the steady Navier–Stokes equations. This was the approach taken by Mullin, Tavener, and Cliffe¹⁰ who investigated the effects of including a central axisymmetric cylinder in the flow numerically. They found that the parameter range for the appearance of a single recirculation bubble was relatively unchanged despite the qualitative change in the boundary conditions. This result is in agreement with the earlier work of Tsitverblit and Kit¹¹ and is also in accord with results of Jahnke and Valentine¹² on a related flow problem.

In the investigation reported here we have developed our earlier work on the variant of the original Vogel problem, where we introduced an inner axial cylinder which now may be either rotating or stationary. The present study is concerned with extending the parameter range of the previous numerical results and carrying out comparisons with complementary experiments. We then introduce a novel aspect and

^{a)} Author to whom correspondence should be addressed. Electronic mail: Tom.Mullin@man.ac.uk

show that sloping the inner boundary can significantly enhance or even suppress the recirculation bubble entirely. These new numerical findings are then substantiated by experiment.

II. EXPERIMENT

Two different sets of experimental apparatus were used in the investigations. In both cases, the outer cylinder and top end plates were held stationary while the bottom wall and inner cylinders were driven round. The first was constructed from a precision ground outer glass cylinder with an inner diameter of 63.5 ± 0.02 mm. A 6.35 ± 0.02 mm diam inner cylinder was located centrally in bearings giving a radius ratio of the two cylinders of 0.1. The bottom wall was attached to the rotating inner cylinder and had a diameter of 63.48 mm while the upper plate was held fixed on a pair of metal rods which could be used to set the aspect ratio of the flow domain. Here we define the aspect ratio Γ to be d/l where $d = r_2 - r_1$, where r_2 is the inner radius of the outer cylinder, r_1 is the radius of the inner and l is the height of the cylindrical gap.

The inner cylinder was driven round by stepper motor via a gearbox and toothed belt drive so that the angular rotation rate of the inner cylinder was known accurately and this was used to estimate the Reynolds number. Here we define the Reynolds number to be $\omega r_1 d / \nu$ where ω is the angular rotation rate of the inner cylinder and ν is the kinematic viscosity of the fluid. The working fluids were water glycerol mixtures whose viscosities were determined using an Ubbelohde viscometer. The outer cylinder was encased in a plexiglass box through which temperature controlled fluid was pumped so that the working section of the experiment was maintained at 28.9°C .

Observations of the flow were made using dye which was injected slowly, close to the inner cylinder, through a small hole in the upper stationary wall. The dye was premixed with the appropriate water-glycerol mixture to minimize any effects it might have on the delicate secondary recirculation. At a given aspect ratio, the bubble first appeared above a certain range of Reynolds numbers. It proved to be extremely difficult to make definite observations of the onset of the bubble since it was a very weak feature and measurements were made difficult by the presence of the adjacent rotating wall. However, once formed, its presence was definite and its disappearance with increase in R proved to be easier to estimate.

The second apparatus was constructed from a plexiglass outer cylinder of inner diameter 140 mm. The inner cylinder was conical such that its diameter varied linearly from 21 mm at the stationary end to 7 mm at the rotating plate. The radius of the inner cylinder was 7 mm at mid-height and we used this dimension to define the radius ratio η to be 0.1 in accord with the numerical investigations discussed below. The height of the fluid domain was fixed at 96 mm so that the aspect ratio was 1.524 where the gap width at mid-height was used as the length scale. The inner cylinder was driven round by a powerful dc (direct current) servo controlled motor and the speed of rotation was calibrated so that the Rey-

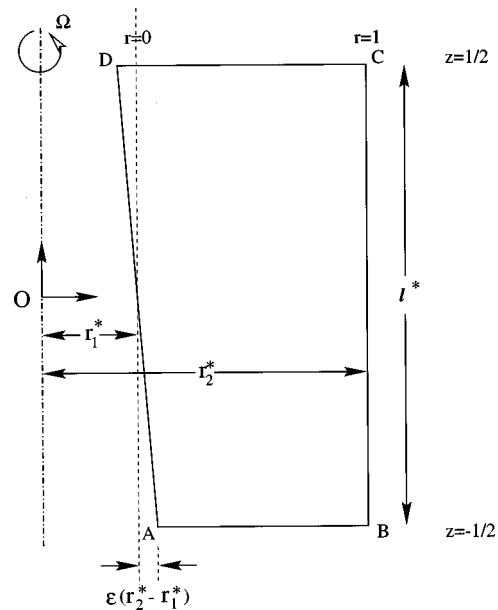


FIG. 1. Schematic of the computational domain.

nolds numbers could be calculated. Observation of the flow reversal was much easier in this case and the flow structure could be seen straightforwardly using a sheet of light, suitable flow visualization particles and viewing from the front. Examples of Taylor-Couette flows visualised in this way may be found in Benjamin and Mullin.¹³

III. GEOMETRY AND NUMERICAL TECHNIQUE

The flows considered here were all confined between a pair of concentric cylinders. The bottom end wall was rotated in every case and the effects of both stationary and rotating inner cylinders were investigated. In addition, we considered the effects of a linear slope on the inner cylinder in both directions. Every combination of rotating-stationary and sloped-straight cylinder was investigated and particular cases will be identified in the discussion of the results. We computed steady, axisymmetric flows of an incompressible Newtonian fluid in bounded annular domains using the numerical routines in the code ENTWIFE. We have considerable experience using these methods in calculations of bifurcations in Navier-Stokes flows, and hence, chose to use this numerical approach despite there being no steady bifurcations in the present problem. The restriction to axisymmetric flows enabled the computations to be performed in two-dimensional (radial) domains, as shown schematically in Fig. 1 where superscripts (*) denote dimensional quantities. We provide an example of a sloped inner cylinder in Fig. 1 for convenience. Here the value of r_1^* used to define the Reynolds number, gap width and radius ratio was the value at the mid-height of the inner cylinder. Clearly $r_1^* - \epsilon(r_2^* - r_1^*) > 0$, hence $\epsilon < \eta / (1 - \eta)$.

The primitive variable formulation of the incompressible steady, axisymmetric Navier-Stokes equations was solved via the finite-element method, using quadrilateral elements

with biquadratic interpolation of the velocity field and discontinuous piecewise linear interpolation of the pressure field.

The length and velocity scales chosen were the gap width $d^* = r_2^* - r_1^*$ and Ωr_1^* , respectively. The Reynolds number was then $R = \Omega r_1^* d^* / \nu$, the aspect ratio, $\Gamma = l^* / d^*$, and the radius ratio $\eta = r_1^* / r_2^*$. In all cases, the value of r_1^* at the mid-height of the cylinders was used in the definition of scales when the inner cylinder was sloped. We defined $r = (r^* - r_1^*) / d^*$, $z = z^* / \Gamma d^*$, $u_r = \Gamma u_r^* / \Omega r_1^*$, $u_\theta = u_\theta^* / \Omega r_1^*$, and $u_z = u_z^* / \Omega r_1^*$.

The boundary conditions applied for a stationary inner cylinder were

$$\begin{cases} u_r = 0 \\ u_\theta = 1 + \left(\frac{1-\eta}{\eta}\right)r, \text{ on } AB, \\ u_z = 0 \end{cases}$$

$$\begin{cases} u_r = 0 \\ u_\theta = 0, \text{ on } BC, CD, \text{ and } DA. \\ u_z = 0 \end{cases}$$

The boundary conditions applied for a rotating inner cylinder were

$$\begin{cases} u_r = 0 \\ u_\theta = 1 + \left(\frac{1-\eta}{\eta}\right)r, \text{ on } AB \text{ and } DA, \\ u_z = 0 \end{cases}$$

$$\begin{cases} u_r = 0 \\ u_\theta = 0, \text{ on } BC \text{ and } CD. \\ u_z = 0 \end{cases}$$

The numerical calculations were carried out on meshes of 25×28 elements. It was found that doubling the number of elements in each direction changed the Reynolds number at which the bubble appeared by $< 0.5\%$. Appropriate corner refinement of the finite-element mesh and smoothing of the velocity discontinuities was employed. Details of both may be found in Tavener, Mullin, and Cliffe.¹⁴ Arclength continuation methods were used to follow solution branches in (R, Γ, η) parameter space. When appropriate, the streamfunction was computed from the primitive variable solution.

IV. RESULTS

The numerical and experimental results will be presented and discussed together. First we will describe the criterion used to distinguish between those parameter regions where a recirculation bubble is deemed to exist and those where it is absent. Then the numerical and experimental results for a right circular cylindrical domain with a straight inner cylinder will be presented and this will be followed by an account of the effect of sloping the inner wall.

A. Criterion for bubble

The onset of the recirculation bubble is a continuous process with increase of R and so an estimate of its appear-

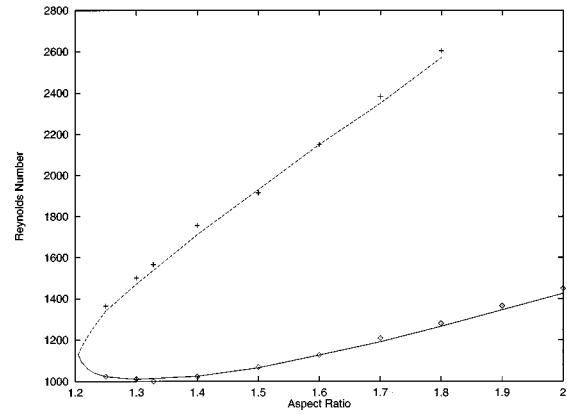


FIG. 2. Comparison between numerical results and experimental results taken from Escudier (1984) for the case where there is no inner cylinder.

ance requires a pragmatic criterion. This was not a straightforward procedure in the experiments since the bubble can only be observed at some small but finite excess R above the creation of the stagnation point. In the numerical calculations, the parameter range of existence of the bubble can be more readily defined by the appearance and disappearance of the stagnation point on the vortex core. The maximum absolute value of the streamfunction of the bubble was typically three orders of magnitude smaller than that of the primary vortex and the spatial location at which it appeared depended on Γ . The weakness of the bubble is often not discussed in the literature where streamlines for the primary and secondary vortices are usually plotted using nonuniform scaling to emphasize the bubble. The fragile nature of the bubble tested the limits of numerical resolution since incipient recirculations were always present in the corners of the domain of calculation. In addition, the spatial location for the appearance and disappearance of the bubble were not the same when R was increased. The bubble usually appeared near the centerline and progressed towards the upper inside corner with increase in R where it disappeared. All of these details made the automatic detection of the parameter range for the existence of the bubble troublesome. Hence we adopted the following pragmatic approach.

The method we used in the numerical work to estimate the first onset of the bubble was to simply visually inspect the streamline plots calculated for fixed Γ when R was increased in steps of $\sim 1\%$. A bubble was deemed to be present when a visible area was first enclosed by the zero streamline. In practice, the bubble grows rapidly with R and sharp estimates could be obtained quite readily and repeatably. Similarly, the disappearance of the bubble was equally rapid with further increase in R and so an estimate of this could also be found with confidence. In order to test the reliability of our methods, we show in Fig. 2 our numerical results for the case when there is no inner cylinder present in comparison with data points taken from Escudier's published experimental results. It can be seen that there is very good agreement between the two and so we are confident in both our numerical techniques and the method for estimating the appearance and

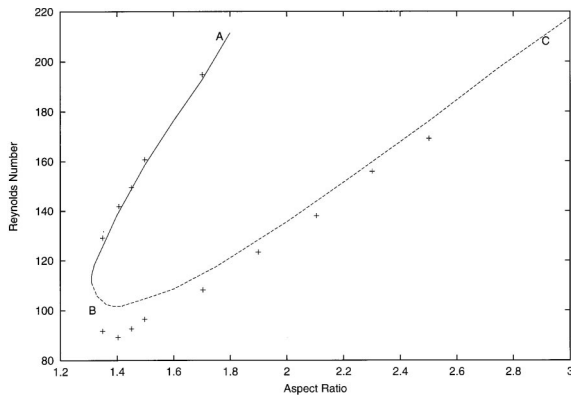


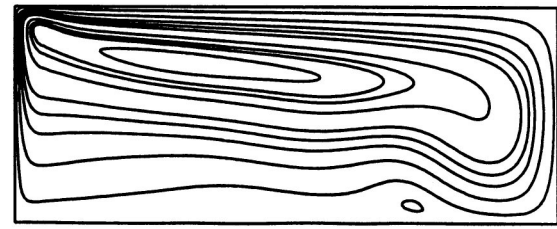
FIG. 3. Comparison between experimental and numerical results for the parameter range of existence of a single recirculation bubble when a small inner cylinder is present. *ABC* is drawn through the calculated results and the experimental points are given by the symbol “+.” The bubble appeared when *R* was increased above *AB* and disappeared when it was increased above *BC*.

disappearance of the recirculation bubble. [N.B. Here $R = \Omega(r_2^*)^2/\nu$.]

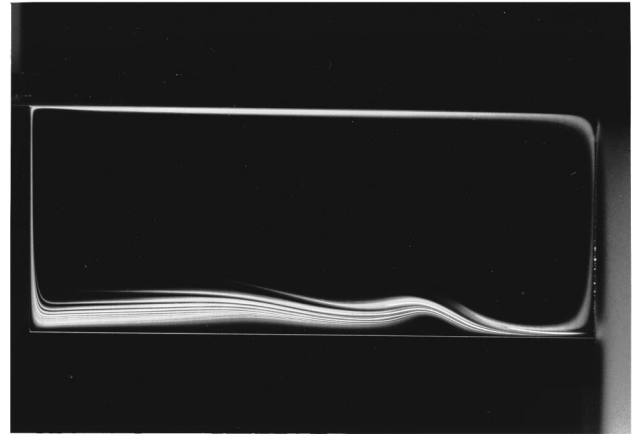
B. Straight inner cylinder

These experimental results were obtained with the precision apparatus described above where the radius ratio was 0.1. The comparison between the experimental and numerical results is presented in Fig. 3 where we have plotted the region of existence of a recirculation bubble in the (R, Γ) plane. The line *ABC* connects the numerical data points obtained using the method described in the previous section. Hence the bubble first appears above *BC* and disappears when *R* is further increased above *AB*. The experimental points are denoted by the symbol “+.” There is excellent agreement between the two for estimates of the disappearance of the bubble but the experimental results are consistently below the numerical ones for the onset of the bubble. This is because it was troublesome to find a reliable measure for the onset in the experiments. As discussed above, the recirculation was weak and since it arose adjacent to the rotating inner cylinder this added to observational difficulties. In fact, distortion of the dye field was often seen before flow reversal adjacent to the inner cylinder could be detected and we suspect this is why the experimental estimates are below the numerical curve. Curiously, the disappearance of the bubble with further increase in *R* was found more reliably in the experiments. Given the excellent agreement between our numerical results and those from Escudier’s experiments shown in Fig. 2 we conclude that the disagreement in the case with the cylinder arises from the difficulties with the observations described above.

An example of a flow with a recirculation is shown in Fig. 4 where we show a comparison between a numerical streamline plot and a cross-sectional flow-visualization. These results were obtained for $\Gamma = 2.5$ and $R = 208$. The distortion of the dye streaks is clearly visible but the maximum absolute value of the streamfunction in the recirculation bubble is $\sim 10^{-3}$ times that of the main vortex as in the case without a cylinder. Next we show in Fig. 5 a series of



(a)



(b)

FIG. 4. A comparison between (a) a numerical streamline plot and (b) an experimental dye visualization for $\Gamma = 2.5$ and $R = 208$.

streamline plots which illustrate a typical sequence for the appearance and disappearance of the recirculation bubble at $\Gamma = 1.6$. As noted in the caption, we have used different scales for the streamlines of the primary and secondary vortices to emphasize the bubble. For this aspect ratio the recirculation bubble first appears near the mid-plane at $R \approx 104$ and disappears at $R \approx 168$ near the top inside corner.

The main conclusion which can be drawn from these results is that the onset of the recirculation bubble is mainly unaffected by the presence of a small straight rotating inner cylinder. One obvious extension to this work would be to either differentially rotate or even stop the inner cylinder. We found that making the inner cylinder stationary had no qualitative effect of the results. The effect of radius ratio of the cylinders was also investigated and it was found that if $\eta \leq 0.1$ then the presence of an inner cylinder had little effect on the flow. Both of these points were established numerically and the detailed results are discussed in Mullin *et al.*¹⁰

C. Sloped inner cylinder

The above results suggest that the flow is unaffected by the presence of a small inner straight cylinder. This is surprising since the inner boundary condition for the flow has been drastically changed from a free core to no-slip. The aim of the next part of the investigation was to study the effect of modifying the axial pressure gradient by sloping the inner cylinder for both stationary and rotating inner cylinders.

The first case we discuss is where the inner cylinder was rotated with the moving lower plate. The inner cylinder had the form of an inverted cone so that the radial gap was wider

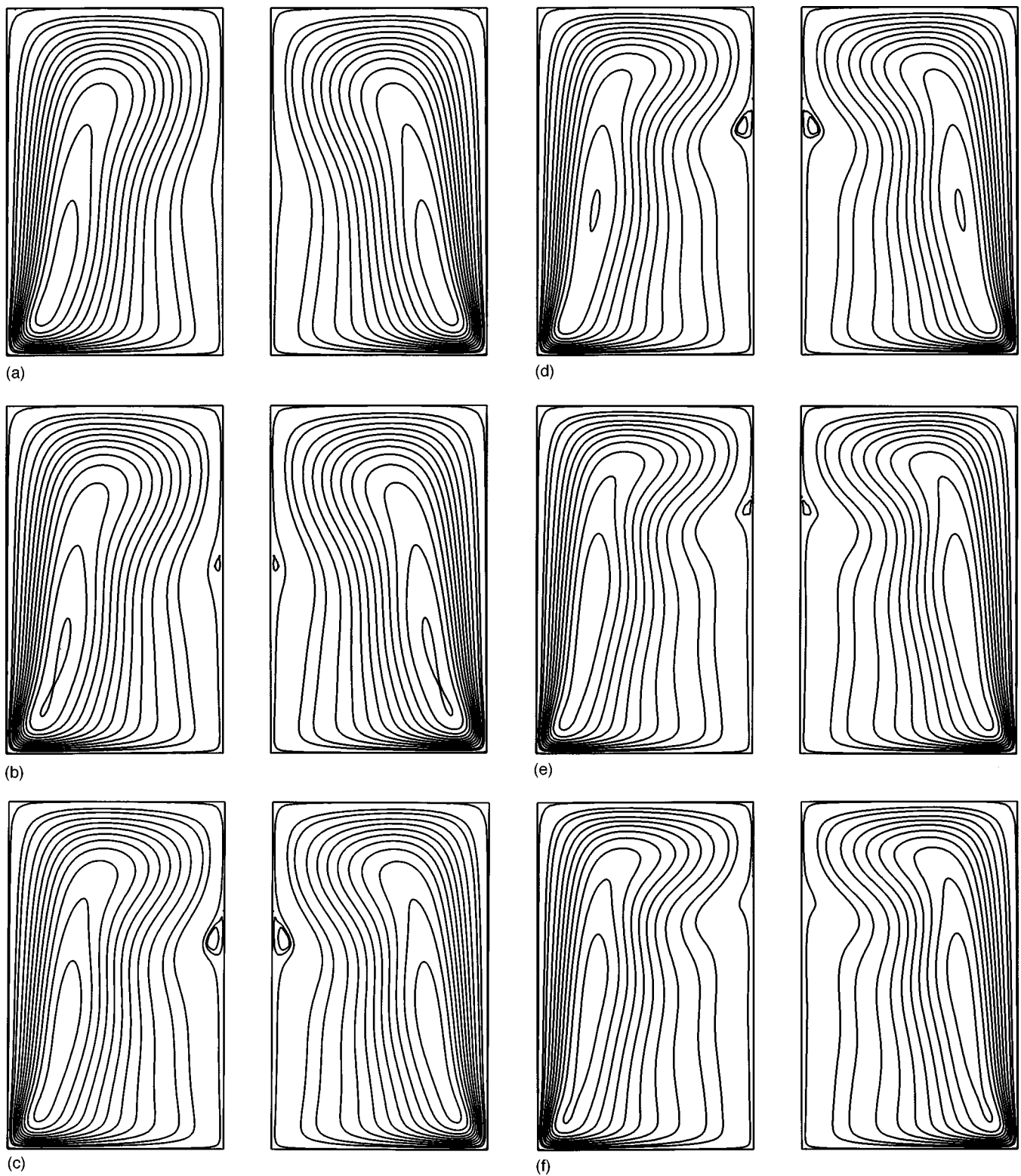


FIG. 5. A “typical” set of streamline plots showing the appearance and disappearance of the recirculation as R is increased at $\Gamma = 1.6$. $\psi = 0$ to 0.12×0.01 , $-0.000\ 03$ and $-0.000\ 005$. (a) $R = 100$. (b) $R = 110$. (c) $R = 130$. (d) $R = 150$. (e) $R = 170$. (f) $R = 180$.

at the bottom than at the top. A comparison between the calculated streamlines and flow visualization photograph is presented in Fig. 6 for the parameter values $(R, \Gamma) = (86.2, 1.524)$. It may be seen immediately that the recirculation is considerably enhanced compared with the straight cylinder case discussed in the previous section. In fact, the

bubble the maximum value of the streamfunction is now an order of magnitude stronger than in the straight cylinder case and it is thus very evident. The bubble first appears at $R = 57.5$ which is approximately half the value for the equivalent aspect ratio with a straight cylinder.

The effect of sloping the inner cylinder is shown graphi-

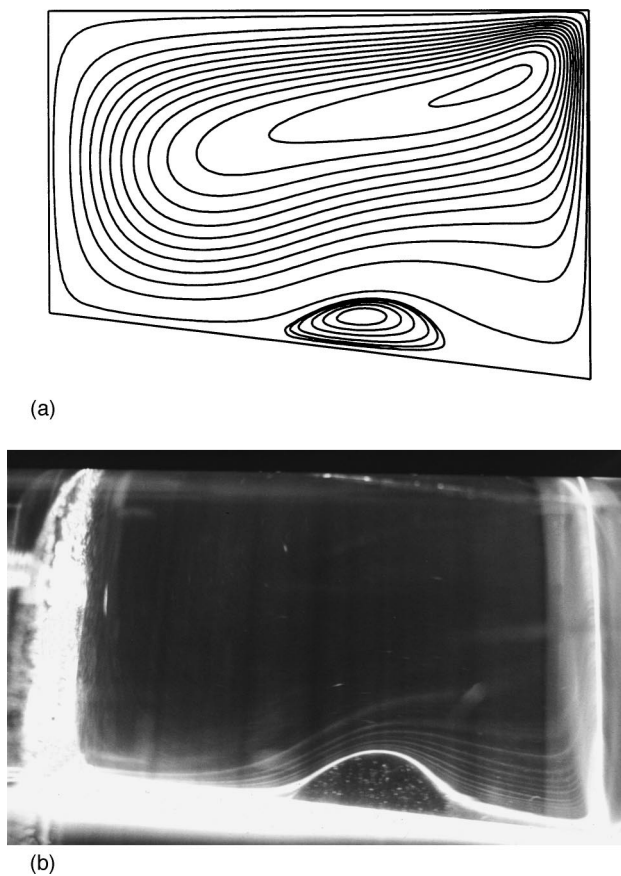


FIG. 6. A comparison between (a) a numerical streamline plot and (b) an experimental flow visualization for a sloped inner cylinder with $\Gamma = 1.524$ and $R = 86.2$. $\psi = 0$ to 0.12×0.01 , -0.00005 , -0.0001 , -0.0002 , -0.0004 , -0.0006 , and -0.0008 .

cally in Fig. 7 where we show a comparison between streamline plots calculated for sloped and straight cylinders at the same parameter values. It is clear that sloping the inner rotating cylinder, such that the gap increased towards the rotating plate enhanced the bubble considerably, whereas when the opposite slope is imposed the recirculation is diminished. The reason for this is that the azimuthal flow adjacent to the rotating wall is greater at the top of the flow domain than at the bottom in the case shown in Fig. 7(a) and this creates an adverse pressure gradient along the inner boundary. The principle circulation driven by the rotating bottom plate is such that the axial flow is downwards adjacent to the inner boundary. Thus, the pressure gradient induced by the sloped rotating wall acts to oppose this motion and the reverse flow of the recirculation is enhanced. When the slope is imposed in the opposite direction as shown in Fig. 7(c) the pressure gradient is favorable and the bubble is suppressed.

We tested this argument further by considering the case where the inner cylinder was stationary. Now the opposite ought to be true since any pressure gradients induced by the inner boundary would be reversed. We show in the streamline plots in Fig. 8 that this is indeed the case. The fluid in the narrower part of the gap adjacent to the stationary inner boundary will be moving more slowly than that below it as in Fig. 8(a) and this will create a favorable pressure gradient which suppresses the recirculation. On the other hand, the

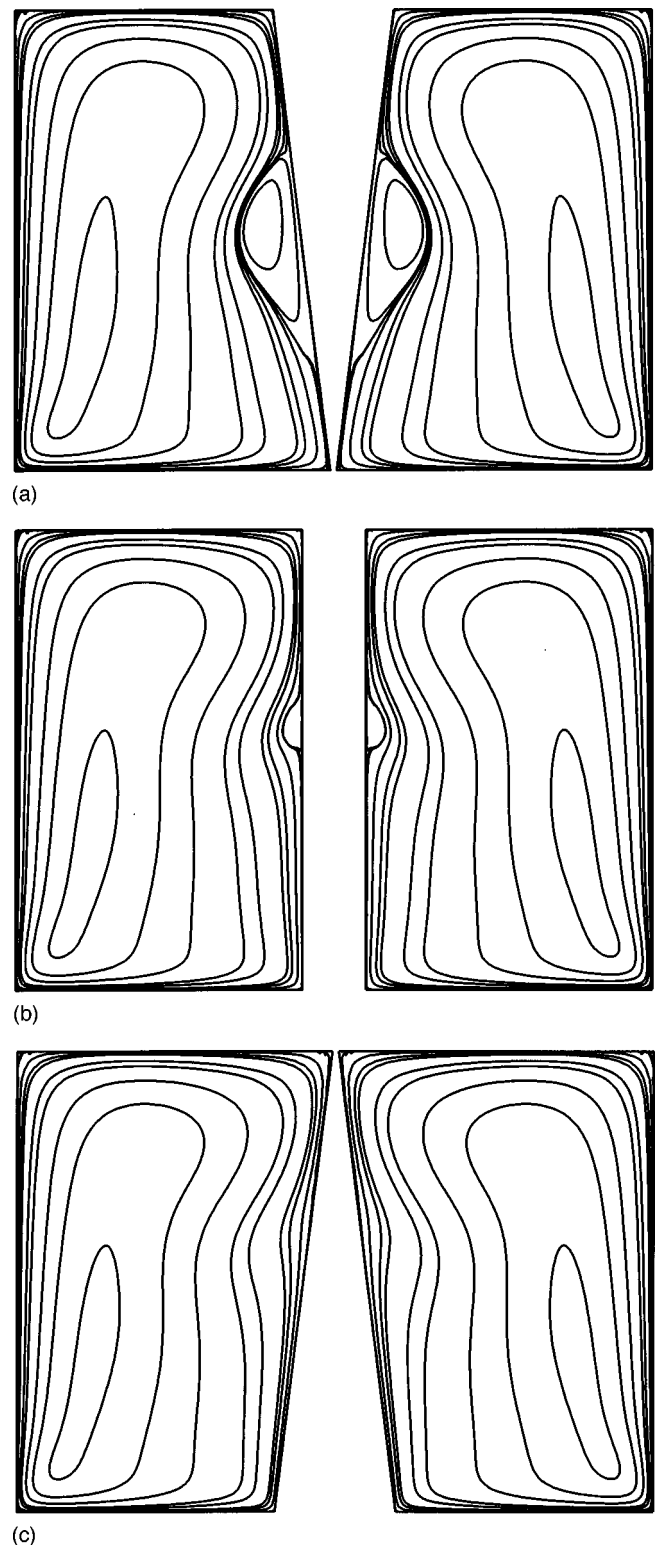
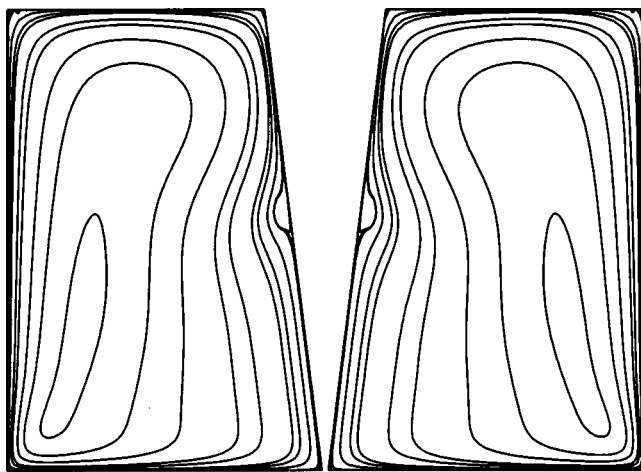
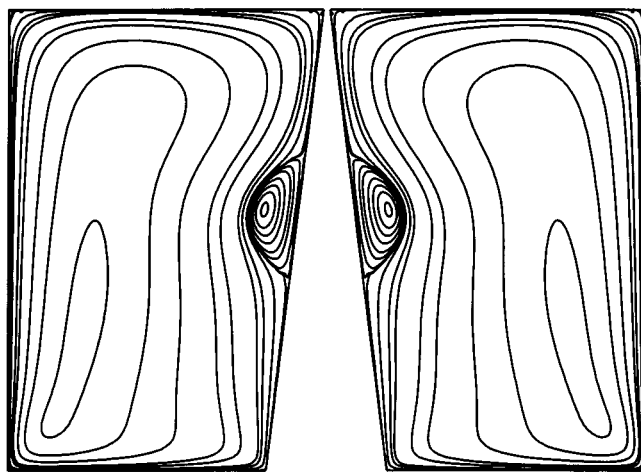


FIG. 7. Streamline plots for the case of a rotating inner cylinder with $\eta = 0.1$, $\Gamma = 1.6$, and $R = 120$. (a) Gap width increasing towards the rotating end. (b) Straight cylinder. (c) Gap width decreasing towards the rotating end. $\psi = 0$ to 0.12×0.01 , -0.00005 , -0.0001 , -0.0002 , -0.0004 , -0.0006 , and -0.0008 .

flow moving downwards into the narrowing decelerating region shown in Fig. 8(b) will experience an adverse pressure gradient which enhances the bubble. Hence rotating and stationary inner cylinders have the opposite effect as predicted.



(a)



(b)

FIG. 8. Streamline plots for the case of a stationary inner cylinder with $\eta = 0.1$, $\Gamma = 1.6$, and $R = 120$. (a) Gap width increasing towards the rotating end. (b) Gap width decreasing towards the rotating end. $\psi = 0$ to 0.001, 0.005, 0.01, 0.03, 0.06, 0.1, $-0.000\ 001$, $-0.000\ 01$, $-0.000\ 05$, -0.0001 , -0.0004 , and -0.0005 .

V. CONCLUSIONS

We have shown that the addition of a small straight cylinder along the centerline of a cylindrical container of fluid

with one rotating wall has no qualitative effect on the appearance of stagnation points on the core of the induced vortex. This is true regardless of whether the central cylinder is rotating or stationary. On the other hand, sloping the inner wall has a dramatic effect on the flow. It arises from a subtle interplay with the pressure gradients at the boundary such that rotating and stationary inner cones with the same slopes have opposite effects on the recirculation bubble.

ACKNOWLEDGMENT

The authors are grateful to Richard Hewitt who first pointed out the pressure gradient arguments to us.

- ¹H. U. Vogel, "Experimentelle Ergebnisse über die laminare Strömung in einem zylindrischen Gehäuse mit darin rotierender Scheibe," *Phys. Fluids* **6**, 2702 (1968).
- ²J. M. Lopez, "Axisymmetric vortex breakdown. Part 1. Confined swirling flow," *J. Fluid Mech.* **221**, 533 (1990).
- ³M. P. Escudier, "Observations of the flow produced by a rotating end wall," *Exp. Fluids* **2**, 189 (1984).
- ⁴N. Tsitverblit, "Vortex breakdown in a cylindrical container in the light of continuation of a steady solution," *Fluid Dyn. Res.* **11**, 19 (1993).
- ⁵N. Tsitverblit and E. Kit, "On the onset of unsteadiness in confined vortex flows," *Fluid Dyn. Res.* **23**, 125 (1999).
- ⁶J. N. Sorensen and E. A. Christensen, "Direct numerical-simulation of rotating fluid-flow in a closed cylinder," *Phys. Fluids* **7**, 764 (1995).
- ⁷A. Spohn, M. Mory, and E. J. Hopfinger, "Observations of vortex breakdown in an open cylindrical container with a rotating bottom," *Exp. Fluids* **14**, 70 (1993).
- ⁸D. T. Valentine and C. C. Jahnke, "Flows induced in a cylinder with both end walls rotating," *Phys. Fluids* **6**, 2702 (1994).
- ⁹J. M. Lopez, "Unsteady swirling flow in an enclosed cylinder with reflectional symmetry," *Phys. Fluids* **7**, 2700 (1995).
- ¹⁰T. Mullin, S. J. Tavener, and K. A. Cliffe, "On the creation of stagnation points in a rotating flow," *J. Fluids Eng.* **120**, 685 (1998).
- ¹¹N. Tsitverblit and E. Kit, "Numerical study of axisymmetric vortex breakdown," *Acta Mech.* **118**, 79 (1996).
- ¹²C. C. Jahnke and D. T. Valentine, "Boundary layer separation in a rotating container," *Phys. Fluids* **8**, 1408 (1996).
- ¹³T. B. Benjamin and T. Mullin, "Notes on multiplicity of flows in the Taylor-Couette experiments," *J. Fluid Mech.* **121**, 219 (1982).
- ¹⁴S. J. Tavener, T. Mullin, and K. A. Cliffe, "Novel bifurcation phenomena in a rotating annulus," *J. Fluid Mech.* **229**, 483 (1991).